THE JOURNAL OF PHYSICAL CHEMISTRY C

Article

pubs.acs.org/JPCC

Analysis of the CO_2 Chemisorption in Li_5FeO_4, a New High Temperature CO_2 Captor Material. Effect of the CO_2 and O_2 Partial Pressures

Hugo A. Lara-García,[†] Pedro Sanchez-Camacho,[†] Yuhua Duan,[‡] José Ortiz-Landeros,[§] and Heriberto Pfeiffer*[,†]

[†]Instituto de Investigaciones en Materiales, Universidad Nacional Autónoma de México, Circuito exterior s/n, Cd. Universitaria, Del. Coyoacán C.P. 04510, Ciudad de México, Mexico

[‡]National Energy Technology Laboratory, United States Department of Energy, 626 Cochrans Mill Road, Pittsburgh, Pennsylvania 15236, United States

[§]Departamento de Ingeniería en Metalurgia y Materiales, Escuela Superior de Ingeniería Química e Industrias Extractivas, IPN, UPALM, Av. Instituto Politécnico Nacional s/n, CP 07738, Ciudad de México, Mexico

ABSTRACT: Pentalithium ferrite (Li_5FeO_4) was tested as possible CO_2 captor, both by theoretical calculations and experimental measurements. The pristine Li_5FeO_4 compound with orthorhombic structure was synthesized via solid-state reaction and it was structural and microstructurally characterized. Later, sample was heat-treated at temperatures from room temperature to 900 °C under different CO_2 or CO_2−O_2 atmospheres. Li_5FeO_4 exhibits excellent CO_2 chemisorption abilities with a capture capacity about 12.9 mmol/g, which is outstanding in comparison to other previously reported ceramic captors. This material is able to react with CO_2 from 200 °C to approximately 715 °C showing a high kinetic of reaction even at CO_2 partial pressure values as low as 0.2. Additionally, results suggest that oxygen addition does enhance the CO_2 chemisorption on Li_5FeO_4 at temperatures below 700 °C, although oxygen addition seems to favor the desorption process at higher temperatures.

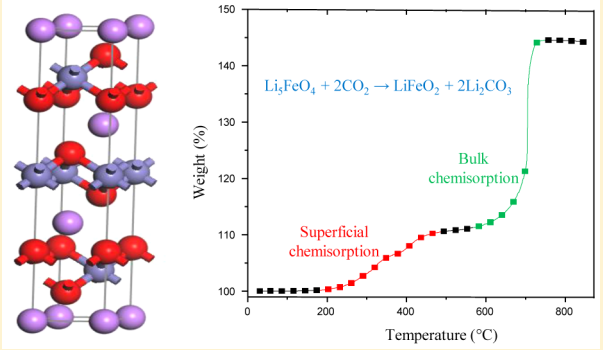

INTRODUCTION

Carbon dioxide is the principal contributor to global warming among the different greenhouse gases (the amount of CO_2 is 80% of greenhouse gases),[1,2] and the emission of this gas into the atmosphere keeps growing. Major CO_2 emission comes from the fossil fuels combustion, which usually has high temperatures. Therefore, carbon capture and storage (CCS) is considered as an option to control CO_2 emissions.[3]

CCS refers to a number of technologies available that capture CO_2 at some stage from the different processes. Nowadays, there are some available technologies for CCS which include postcombustion, precombustion, oxy-fuel combustion, and chemical looping combustion processes.[4] As aforementioned, the major CO_2 emissions are in the form of flue gases from fossil fuel combustion; for that reason, postcombustion is the most studied technology. In this regard, in the last years several materials have been proposed as possible CO_2 captors: amines, hydrotalcites, zeolites, metal−organic frameworks (MOFs), and metal oxides, among others. Some of these materials are used in order to reduce the emissions. However, all of them have some advantages and disadvantages to be considered suitable materials for CCS.[4−8] An ideal capture material should have certain properties, such as large capacity of capture, adequate kinetics, thermal stability, and cyclability among others.[7]

Lithium ceramics are materials that have been recently widely studied as possible CO_2 captors under different physicochemical conditions, where some of them satisfy the properties describe above, for example, lithium zirconates (Li_2ZrO_3, $Li_6Zr_2O_7$),[9−12] lithium silicates (Li_8SiO_6, Li_4SiO_4, Li_2SiO_3),[13−16] lithium aluminate (Li_5AlO_4),[17] lithium cuprate (Li_2CuO_2),[18−20] and lithium titanate (Li_4TiO_4).[21] These ceramics are able to chemisorb CO_2 at high temperatures (400−800 °C), where the CO_2 chemisorption is carried out in two different stages, (i) superficial and (ii) bulk processes. Initially, carbon dioxide reacts with the superficial particles of the lithium ceramic, forming a product shell of lithium carbonate and different secondary phases, depending on the initial lithium ceramic composition. After that, the unreacted lithium ceramic core reacts with CO_2 through different processes but mainly depending of different diffusion mechanisms including the CO_2 diffusion through the external

Received: December 9, 2016
Revised: January 20, 2017
Published: January 23, 2017

DOI: 10.1021/acs.jpcc.6b12431
J. Phys. Chem. C 2017, 121, 3455−3462

carbonate shell, as well as the lattice and grain boundary diffusion of lithium and oxygen.[22,23]

On the other hand, the Li—Fe—O phase diagram reports three ternary compounds, $LiFeO_2$, $LiFe_5O_8$, and Li_5FeO_4.[24] These materials have been used for electrical applications, such as lithium-ion batteries,[25−29] but there are only three reports where $LiFeO_2$ has been tested as CO_2 captor (reaction 1). These reports show that $LiFeO_2$ is able to chemisorb CO_2 between 200 and 500 °C. Nevertheless, it only captures small amounts of CO_2.[30−32] Therefore, the aim of this work was to evaluate, theoretically and experimentally, a different lithium ferrite composition, the pentalithium ferrite (Li_5FeO_4), as a possible CO_2 material captor under different physicochemical conditions, according to the following reaction (reaction 2)

$$2LiFeO_2 + CO_2 \rightarrow Li_2CO_3 + Fe_2O_3 \quad (1)$$

$$0.5Li_5FeO_4 + CO_2 \rightarrow Li_2CO_3 + 0.5LiFeO_2 \quad (2)$$

where the maximum CO_2 amount that Li_5FeO_4 can chemisorb is equal to 12.9 mmol of CO_2 per gram of ceramic. Of course, this value is importantly higher in comparison to the $LiFeO_2$−CO_2 reaction system, where the maximum chemisorption is 5.2 mmol of CO_2 per gram of $LiFeO_2$.

EXPERIMENTAL SECTION

Pentalithium ferrite (Li_5FeO_4) was synthesized by solid state reaction using lithium oxide (Li_2O, Aldrich) and iron oxide (Fe_2O_3, Aldrich). Initially, the powders were mechanically mixed and pressed into pellets (15 MPa). Subsequently, the pellets were heated to 850 °C for 20 h. Twenty mol % of Li_2O excess was used due to its tendency to sublimate.

After the Li_5FeO_4 synthesis, the sample was structural and microstructurally characterized. For the structural characterization, X-ray diffraction (XRD) pattern was obtained from a diffractometer (Siemens D5000) coupled to a cobalt anode X-ray tube. Li_5FeO_4 crystalline phase was identified using the Joint Committee Powder Diffraction Standards (JCPDS) database. On the other hand, some microstructural features were determined by N_2 adsorption−desorption measurements, where the surface area was determined using the Brunauer−Emmett−Teller (BET) model. This analysis was performed using a Minisorp II instrument from Bel-Japan. The experiment was performed at 77 K, using a multipoint technique, where the sample was previously degassed at room temperature for 24 h in vacuum.

After the sample characterization, different thermal analyses were performed using a Q500HR instrument from TA Instruments. Initially, the Li_5FeO_4 sample was dynamically heated from room temperature to 850 at 5 °C/min, using different CO_2 or CO_2−O_2 partial pressures (CO_2 Praxair grade 3.0 and O_2 Praxair grade 3.0) N_2 balanced (Praxair, grade 4.8), where the total flow rate was 60 mL/min in all the cases. The P_{CO2} and P_{O2} were determined by their fraction of the total feed flow rate and the total pressure. Afterward, different isothermal analyses were performed between 350 and 800 °C, using different P_{CO2} and P_{O2} values N_2 balanced. For the isothermal experiments, each sample was heated to the corresponding temperature into a N_2 flow. Then, once the temperature was reached, the gas was switched from N_2 to the different P_{CO2} and P_{O2}. Moreover, all the isothermal products were recharacterized by XRD in order to elucidate the different carbonation products.

To better understand the experimental results, the ab initio thermodynamic calculations, by combining density functional theory (DFT) with lattice phonon dynamics, were performed on the Li_5FeO_4—CO_2 and $LiFeO_2$—CO_2 systems. The detailed description of the calculation method can be found in previous studies.[33−35] In addition, Figure 1 shows the

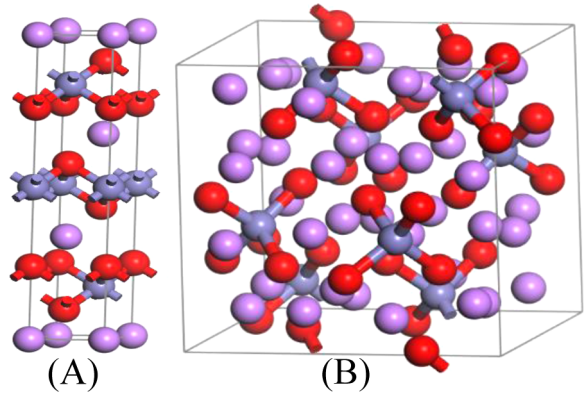

Figure 1. Li_5FeO_4 (A) and $LiFeO_2$ (B) crystal structures involved in the CO_2 carbonation process. Red ball stands for oxygen, purple stands for lithium, and gray stands for iron atoms (*c*-axis is vertical).

Li_5FeO_4 (1-A) and $LiFeO_2$ (1-B) crystallographic structures used for the thermodynamic analysis: The Li_5FeO_4 orthorhombic structure with space group *Pbca* (#61) and the $LiFeO_2$ trigonal structure with space group $R\bar{3}mH$ (#166).[36,37] The Vienna ab initio simulation package (VASP[38,39]) was used to optimize the lithium ferrite structures in order to obtain their DFT energies. Then, the corresponding supercells were created for phonon calculations. In the phonon calculations, displacements of 0.03 Å of nonequivalent atoms were generated. After that, DFT calculations were performed again to obtain the force on each atom due to displacements. These forces are carried back to PHONON package[40] to calculate the phonon dispersions and densities from which the partition function can be carried out and used to obtain free energies and entropies. From the calculated DFT energy, phonon free energy, and entropy of each reactant and product, the thermodynamic properties ($\Delta H(T)$, $\Delta G(T)$, $\Delta S(T)$, and the temperature-CO_2 pressure relationship) can be obtained and used for evaluating the CO_2 capture reactions 1 and 2 by Li_5FeO_4 and $LiFeO_2$.

RESULTS AND DISCUSSION

Figure 2 shows the calculated heat of reaction and free energy change of the reactions 1 and 2. Although both reactions are exothermic processes (Figure 2A) in the analyzed temperature range, when Li_5FeO_4 captures CO_2 it releases almost the double amount of heat in comparison to $LiFeO_2$. Additionally, from the free energy change (Figure 2B) it can be seen that $LiFeO_2$ only can react with CO_2 under T < 250 °C, whereas Li_5FeO_4 can react with CO_2 up to 820 °C. All these data strongly support the Li_5FeO_4 carbonation process. Moreover, Figure 2C shows the relationship between the CO_2 pressure versus temperature for the same reactions. From this curves, it is clearly evident that at postcombustion conditions (P_{CO2} = 0.1) $LiFeO_2$ only can capture CO_2 below 192 °C whereas Li_5FeO_4 performs the carbonation process up to 700 °C. On the other hand, under precombustion conditions Li_5FeO_4 can capture CO_2 up to 970 °C, whereas $LiFeO_2$ only reacts up to

DOI: 10.1021/acs.jpcc.6b12431
J. Phys. Chem. C 2017, 121, 3455−3462

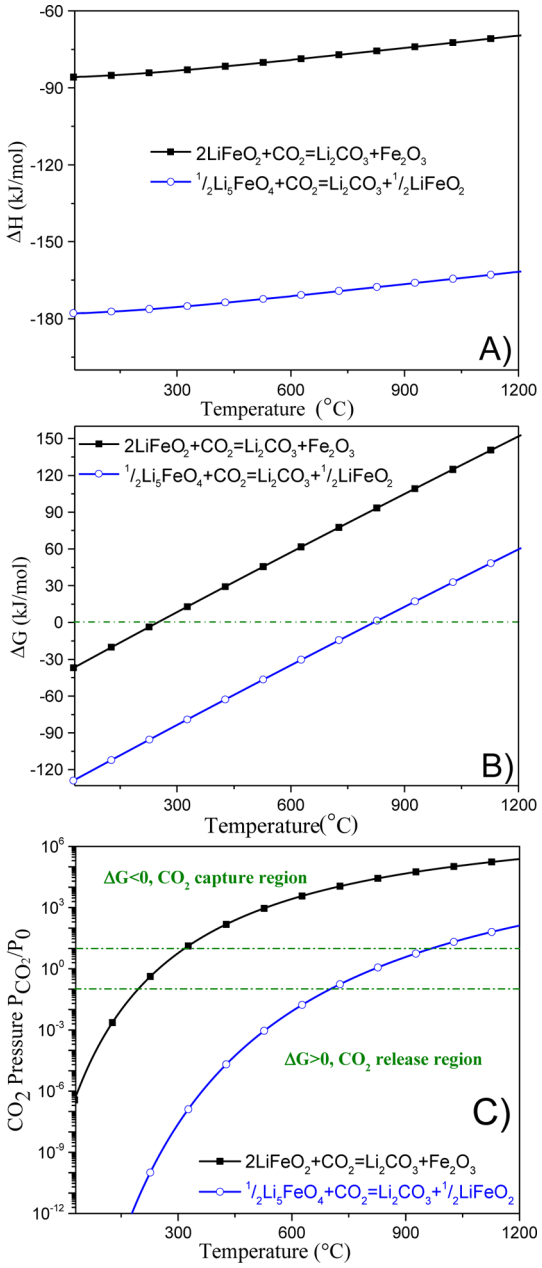

Figure 2. Calculated thermodynamic properties of reactions of Li_5FeO_4 and $LiFeO_2$ capturing CO_2 versus temperatures. (A) Heat of reaction, (B) free energy, and (C) the calculated vant' Hoff plots of the relationships among the free energy (ΔG), temperature (T,) and gas pressure (P in logarithmic scale) for Li_5FeO_4 and $LiFeO_2$. Only $\Delta G = 0$ curves are shown explicitly. $P = P_{CO2}/P_0$, where P_0 is the reference pressure set to 1 bar. For each reaction above the $\Delta G = 0$ curve, the sorbent absorbs CO_2 and the reaction goes forward ($\Delta G < 0$ region) to form Li_2CO_3, whereas below the $\Delta G = 0$ curve, the carbonate releases CO_2 and the reaction goes backward to regenerate the sorbent ($\Delta G > 0$ region).

340 °C. On the basis of these results calculated under different conditions, the Li_5FeO_4 is able to trap CO_2 chemically in a large temperature range, producing Li_2CO_3 and $LiFeO_2$, where $LiFeO_2$ does not present as convenient CO_2 capture conditions, at least thermally.

After the thermodynamic analysis, Li_5FeO_4 was synthesized, characterized, and evaluated as a possible CO_2 captor. Figure 3 shows the XRD pattern of the Li_5FeO_4 fitting with the 00-037-

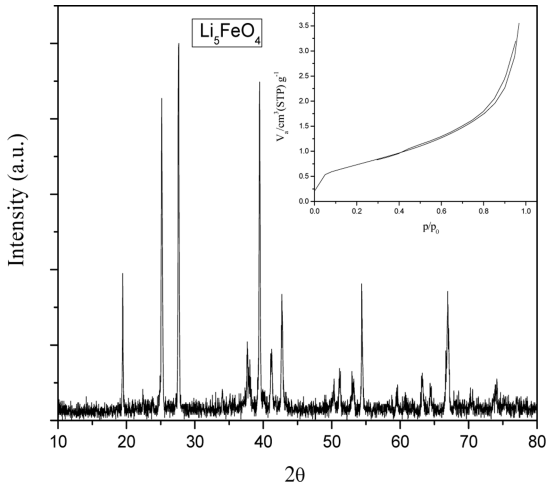

Figure 3. XRD pattern and N_2 adsorption−desorption curve (square inset) of the Li_5FeO_4 sample synthesized by solid state reaction method.

1151 PDF file, the orthorhombic crystalline phase of the pentalithium ferrite. Moreover, the square inset of Figure 3 shows the N_2 adsorption−desorption isotherm for the Li_5FeO_4 sample corresponding to a type II isotherm, usually obtained in nonporous materials.[41] Additionally, the surface area of the sample was estimated to be 2.6 m^2/g using the BET model. This microstructural analysis is in good agreement with the solid-state synthesis method.

After the Li_5FeO_4 characterization, this material was evaluated as CO_2 captor varying different physicochemical conditions, such as temperature, P_{CO2} effect, and the oxygen addition effect into the gas mixture (P_{CO2}−P_{O2}). In this reaction, it has to be assumed that Li_5FeO_4 reacts partially with CO_2, where $LiFeO_2$ does not react with CO_2. In fact, previous papers have shown that $LiFeO_2$ is able to chemisorb very low quantities of CO_2 (<2 wt %) between 200 and 450 °C and after 460 °C the CO_2 desorption occurs.[30−32] Moreover, the negligible $LiFeO_2$ reactivity was probed below during the XRD analysis performed to the Li_5FeO_4 isothermal products.

Therefore, Li_5FeO_4 is able to trap 12.9 mmol of CO_2 per gram of ceramic, considering that $LiFeO_2$ does not contribute to the CO_2 chemisorption. Figure 4 shows the dynamic thermogravimetric analysis of the Li_5FeO_4 in the presence of a saturated CO_2 atmosphere. As reported for other lithium and sodium ceramic,[22,23] the CO_2 chemisorption was divided in two different temperature ranges, from 205 to 480 °C and from 600 to 715 °C. The first weight increment corresponds to the superficial CO_2 chemisorption process, where a complete Li_2CO_3−$LiFeO_2$ external shell is produced covering the Li_5FeO_4. Then, CO_2 chemisorption is only reactivated when different diffusion processes are thermally activated. Thus, the bulk CO_2 chemisorption is produced during the second weight increment observed in the dynamic thermogram.

Although the general behavior presented in the Li_5FeO_4−CO_2 system was similar to other lithium-based materials, the superficial CO_2 chemisorption presented here showed some fluctuations as it was evidenced in the DTG curve. The formation of these variations may be attributed to different factors such as a partial sintering, the CO_2 chemisorption−desorption of $LiFeO_2$, and thermal Li_5FeO_4 phase transformation processes.

DOI: 10.1021/acs.jpcc.6b12431
J. Phys. Chem. C 2017, 121, 3455−3462

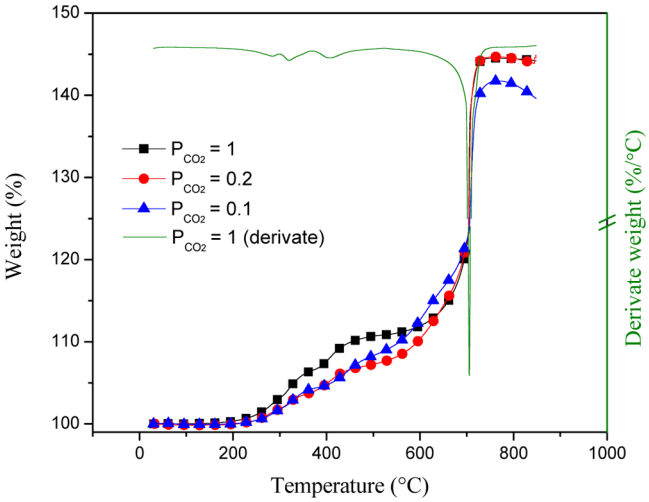

Figure 4. Dynamic TG and DTG curves of the Li_5FeO_4 in a saturated CO_2 atmosphere (60 mL/min). In addition, the dynamic TG curves of the of the Li_5FeO_4 using different P_{CO2} are presented.

All these effects may induce variations on the surface availability modifying the CO_2 capture and consequently the weight gained, qualitatively. In fact, these effects are in good agreement with the literature ($LiFeO_2$–CO_2 chemisorption–desorption[30−32]) or evidenced in the present work (sintering and phase transitions) during the isothermal analysis and the isothermal products characterization.

On the basis of the previous results other dynamic thermograms were performed with different P_{CO2} in the absence and presence of oxygen (P_{O2} = 0.05), all of them N_2 balanced. The same Figure 4 shows the CO_2 chemisorption dynamic thermograms with P_{CO2} of 0.1 and 0.2. It is clearly evident that these thermogram trends did not vary in comparison to the CO_2 saturated atmosphere curve. Perhaps, the main difference observed in these thermograms is that the superficial CO_2 chemisorption produced between 230 and 480 °C was not as efficient as in the CO_2 saturated atmosphere. Moreover, using the lowest P_{CO2} showed some thermal shift during the bulk CO_2 chemisorption process and the CO_2 desorption process was activated at lower temperatures. These effects may be attributed to CO_2 sorption–desorption equilibrium changes produced in the solid–gas interface due to the CO_2 concentration. Besides, the effect of the oxygen addition was evaluated on the same thermal and CO_2 concentration conditions. Thus, Figure 5 shows the dynamic thermogravimetric curves with the CO_2 concentrated (P_{CO2} = 1.0) and with only a P_{CO2} of 0.2, both in the presence of a P_{O2} equal to 0.05. In these cases, the oxygen addition seemed to have a more evident effect when P_{CO2} was equal to 0.2. In this case, there were some temperature ranges (320–410 °C and 430 and 605 °C) where the CO_2 capture was qualitatively improved due to the oxygen addition. Both oxygen improvements seem to be at a superficial level, before the different diffusion process are activated. Therefore, in order to further analyze the P_{CO2} and P_{CO2}–P_{O2} effects different isothermal analyses were performed.

Figure 6 shows the four isothermal sets where the carbon dioxide concentration is analyzed in the absence or presence of oxygen. The Li_5FeO_4 carbonation process into a saturated CO_2 atmosphere is shown in the Figure 6A and as it could be expected all the isotherms presented an exponential behavior. Nevertheless, isotherms were visually separated in two different groups, depending on temperature: from 350 to 650 °C and from 700 to 800 °C. The lowest temperature used was 350 °C, where the final weight increment was 6.4 wt %. Then, at 400 °C the final weight increment was not so different, 6.8 wt %, although the exponential trend did vary in comparison to the previous isotherm. At 400 °C, most of the weight increment was produced during the first reaction moments (~10 min), while at 350 °C the chemisorption was produced much more slowly. This chemisorption behavior confirmed that Li_5FeO_4–CO_2 reactivity is increased as a function of temperature, but as the diffusion processes have not been thermally activated the carbonation is limited to the initial surface area, being it the same in both cases. On the contrary, when temperature was increased to 500 °C the carbonation seemed to be as fast as at 400 °C during the first reaction moments but the final weight increment was decreased to only 5 wt %. These results indicate a partial Li_5FeO_4 sinter during the initial heating process, diminishing the surface area and consequently the sample carbonation. Isotherms performed at 600 and 650 °C increased their final weight increments to 9.7 and 17.9 wt %, meaning that the diffusion process has been partially activated in this temperature range. Consequently, the Li_5FeO_4 sintering process is no longer important. Actually, after these temperature isotherms presented the second visual behavior, almost all the CO_2 chemisorption was produced in the first reaction moments and the final weight increments were high. Between

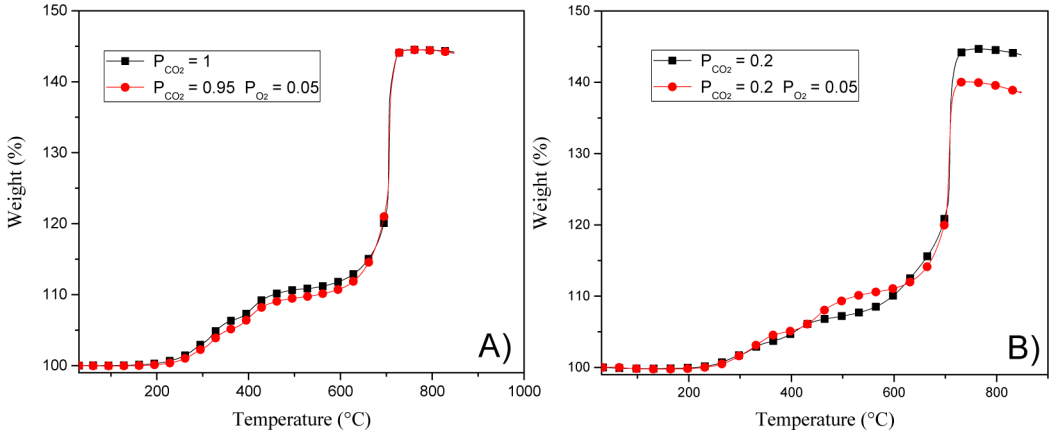

Figure 5. Dynamic TG curves of the Li_5FeO_4 using different CO_2–O_2 gas mixtures.

DOI: 10.1021/acs.jpcc.6b12431
J. Phys. Chem. C 2017, 121, 3455−3462

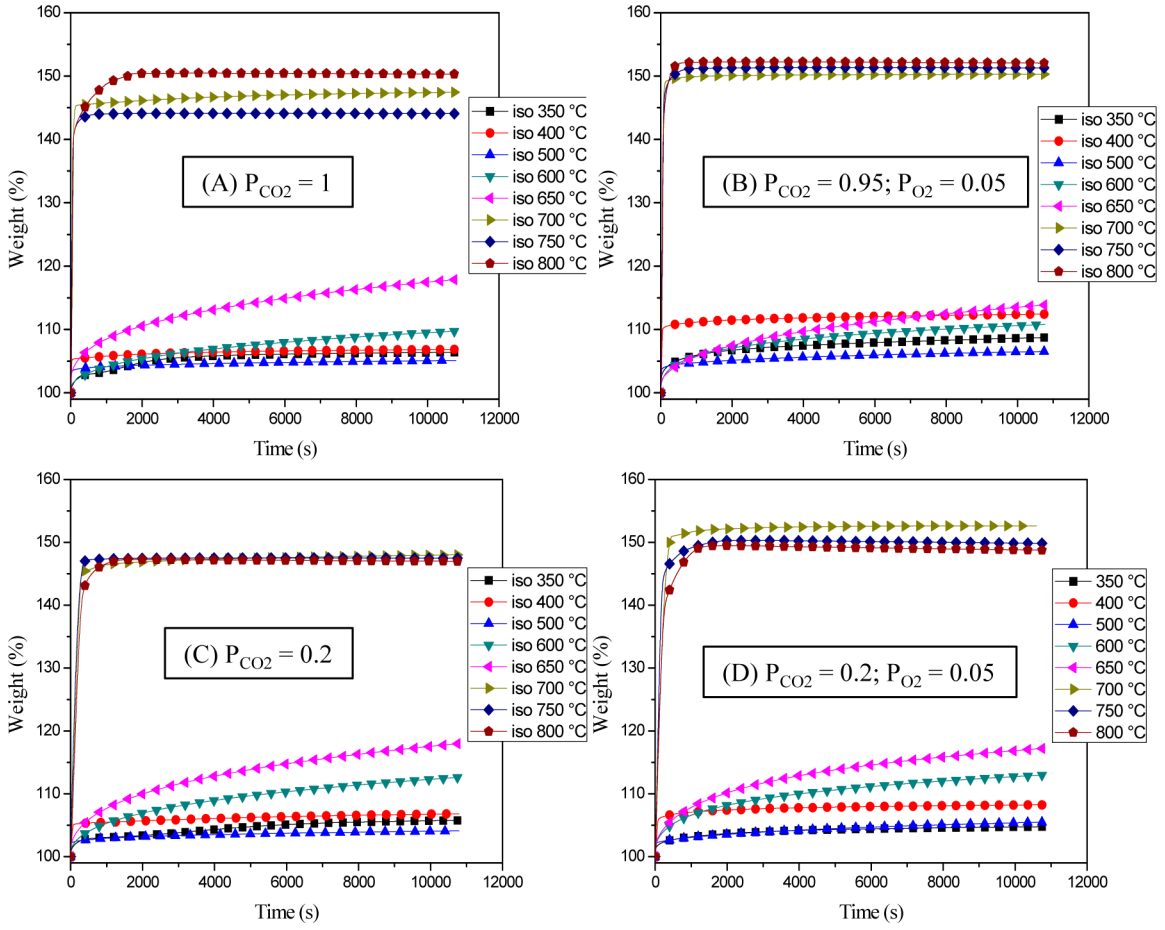

Figure 6. Isothermal TG curves of the Li_5FeO_4 using two different P_{CO2} partial pressures (1.0 or 0.2) in the presence and absence of oxygen (P_{O2} was 0 or 0.05).

700 and 800 °C, the final weight increments were 47.4, 44, and 50.3 wt %, although the variations observed in this temperature range could be attributed to different factors as the lithium carbonate melting process and the decarbonation equilibrium activation. In the first case, Li_2CO_3 melting may favor the CO_2 diffusion, enhancing the Li_5FeO_4 carbonation. On the contrary, the decarbonation activation must establish different Li_5FeO_4–CO_2 carbonation–decarbonation equilibriums as a function of temperature.

All the other isothermal sets presented very similar general behaviors, as it is summarized in the Figure 7, where the final isothermal weight increments are presented. All the isothermal sets presented two different weight increment trends: between 350 and 650 °C and between 700 to 800 °C. Additionally, Li_5FeO_4 tends to sinter, diminishing its surface area, at around 500 °C. Nevertheless, there are some specific differences among the isothermal sets that must be pointed out. When the isotherms were performed using a P_{CO2} = 0.2 (Figure 6B), the CO_2 chemisorption was very similar to that previously described for the P_{CO2} = 1, which means low concentration of CO_2 does not decrease the capture capacity in lithium ferrite, at least qualitatively. Moreover, if oxygen was added to the isotherms (Figure 6C,D) the final weight increments were improved, as can seen in Figure 7. In this figure, the final weight increments were higher in the isotherms performed in the oxygen presence at almost any temperature. Additionally, the kinetics seems to be highly improved as well, as it is evidenced during the first minutes of the isotherms performed at 400 °C

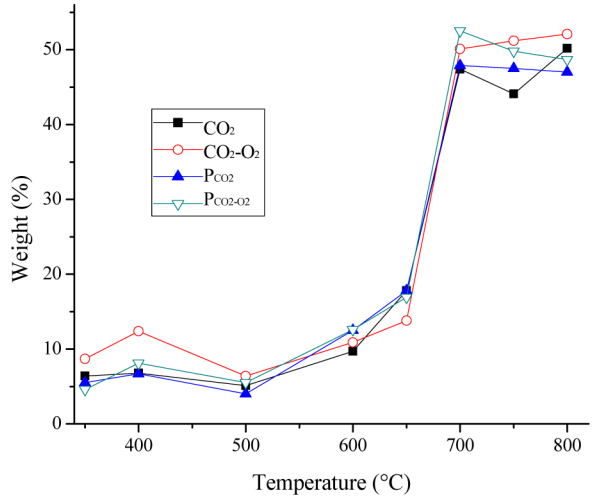

Figure 7. Evolution of the final weight increments observed after the Li_5FeO_4 carbonation process at different temperatures, varying the CO_2 and O_2 partial pressures.

(this assumption is going to be attested below). It is worth noting that using a P_{CO2} = 0.2 in the presence of oxygen the maximum capture is reached at 700 °C; after this temperature, the chemisorption decreases as a function of the temperature, which means that oxygen seems to favor the desorption process.

DOI: 10.1021/acs.jpcc.6b12431
J. Phys. Chem. C 2017, 121, 3455–3462

All these results clearly show that Li_5FeO_4 has a high CO_2 chemisorption capacity at high temperatures; specifically, this material presents very good CO_2 captures between 700 and 800 °C under different gas concentrations. Within this context, Li_5FeO_4 presents as high CO_2 chemisorption capacities as other alkaline ceramics, such as Li_8SiO_6,[13] Li_4SiO_4,[14−16] $Li_6Zr_2O_7$,[42] Li_5AlO_4,[17] Na_2ZrO_3,[43] and $K_2Ti_2O_5$,[44] among others. Moreover, the oxygen addition enhances the CO_2 chemisorption, which may be explained due to the following different factors: (1) oxygen may have been dissociated over the Li_5FeO_4, favoring the formation of carbonate formation or (2) oxygen may have reacted with Li_5FeO_4 producing Li_2O, which consecutively reacted with CO_2 producing the final Li_2CO_3 phase.

After the isothermal experiments, all the isothermal products were recharacterized by XRD. Figure 8 shows the XRD patterns

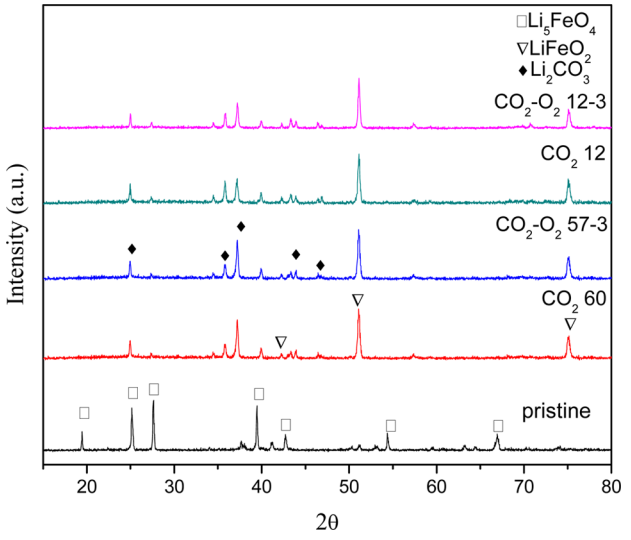

Figure 8. XRD patterns of the Li_5FeO_4 after the isothermal processes performed at 600 °C, varying the CO_2 and O_2 partial pressures. The pristine Li_5FeO_4 was included for comparison purposes.

of all the isothermal products obtained at 700 °C in addition to the pristine Li_5FeO_4 sample for comparison purposes. All these isothermal products showed the formation of lithium carbonate (Li_2CO_3) and a different lithium ferrite ($LiFeO_2$) crystalline phase, which possesses a lower Li/Fe molar ratio than Li_5FeO_4. The $LiFeO_2$ phase was identified with the PDF card No. 00-17-0938. In fact, these products are in very good agreement with the proposed reaction 1. Therefore, 1 mol of Li_5FeO_4 does react with 2 mol of CO_2. These results confirmed that $LiFeO_2$ does not contributed to the CO_2 chemisorption, as it has been probed that $LiFeO_2$ only has a small CO_2 chemisorption−desorption process between 300 and 500 °C.[30−32] Furthermore, these results are in good agreement with the thermodynamic data described above, where the $LiFeO_2$−CO_2 reactivity is limited to temperatures below 250 °C.

On the basis of the Li_5FeO_4−CO_2 reactivity results previously described and in order to further analyze the isothermal curves presented in Figure 6, the CO_2 saturated atmosphere data were fitted to the first order reaction model to respect to Li_5FeO_4, with and without oxygen. This model has been previously used for other alkaline ceramics, where several processes are being produced and therefore only the first moments of the whole mechanism are kinetically analyzed. In other words, only the superficial CO_2 chemisorption is analyzed.[45−47] The rate first order reaction model can be assumed as follows

$$\ln[Li_5FeO_4] = -kt \tag{3}$$

where k is the reaction rate constant, t is the time, and $[Li_5FeO_4]$ corresponds to the molar concentration of the ceramic. The obtained k-values are presented in Table 1. In the $P_{CO2} = 1$ case, and as it could be expected, the k-values tend to increase as a function of temperature, except at temperatures equal or higher than 750 °C. In this temperature range, the CO_2 chemisorption−desorption equilibrium is active, as it was previously described. Thus, the reactivity should have been modified. Additionally, when oxygen ($P_{O2} = 0.05$) was added to the gas flow the k-values again increased as a function of temperature as in the oxygen absence. However, these k-values resulted to be slightly better than those obtained without oxygen. Moreover, only the 750 and 800 °C data presented lower k-values in the absence of oxygen. Finally, both sets of k-values were fitted to the Eyring's model, which is used for heterogeneous reactions 4

$$\ln\left(\frac{k}{T}\right) = \frac{-\Delta H^{\ddagger}}{RT} + \frac{\Delta S^{\ddagger}}{R + C} \tag{4}$$

where are $\Delta H^{\ddagger}$ and $\Delta S^{\ddagger}$ are the activation enthalpy and entropy respectively, T is temperature, k is the rate constant, R is the universal gas constant, and C corresponds to a constant equation value.

Therefore, the k constant values obtained for the Li_5FeO_4−CO_2 system in a certain temperature range were used to determine the activation enthalpy ($\Delta H^{\ddagger}$), in presence and absence of oxygen. Figure 9 shows the corresponding ln k/T versus $1/T$ plots, where the $\Delta H^{\ddagger}$ values obtained were 88.29

Table 1. Kinetic Constant Values Obtained from the First Order Reaction Model for the CO_2 Chemisorption on Li_5FeO_4 into a CO_2 Saturated Atmosphere in the Presence or Absence of Oxygen

	$P_{CO2} = 1.0$			$P_{CO2} = 0.95$ and $P_{O2} = 0.05$		
temp (°C)	k (sec^{-1})	error	R^2	k (sec^{-1})	error	R^2
350	0.00109	1.2823×10^{-5}	0.9974	0.00219	4.9507×10^{-5}	0.9858
400	0.00238	6.6881×10^{-5}	0.9844	0.00231	4.0635×10^{-5}	0.9920
500	0.00233	6.7492×10^{-6}	0.9997	0.00333	4.5013×10^{-5}	0.9954
600	0.00154	2.0361×10^{-5}	0.9968	0.00214	2.3336×10^{-5}	0.9978
650	0.00210	7.9017×10^{-5}	0.9777	0.00260	7.2143×10^{-5}	0.9878
700	0.00424	7.4181×10^{-5}	0.9933	0.00464	5.9921×10^{-5}	0.9963
750	0.01081	2.1963×10^{-4}	0.9909	0.00825	1.6675×10^{-4}	0.9923
800	0.00569	2.0501×10^{-4}	0.9783	0.00761	1.2336×10^{-4}	0.9934

DOI: 10.1021/acs.jpcc.6b12431
J. Phys. Chem. C 2017, 121, 3455−3462

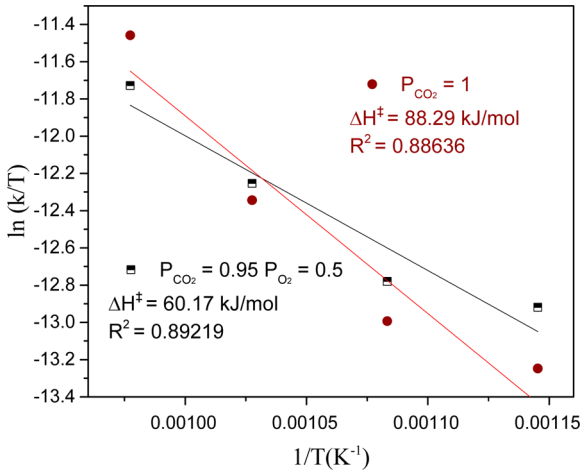

Figure 9. Eyring-type plot of $\ln(k/T)$ versus $1/T$ for data obtained assuming a first-order reaction of Li_5FeO_4, using a CO_2 (P_{CO2} = 1) or CO_2–O_2 (P_{CO2} = 0.95 and P_{O2} = 0.05) atmospheres.

and 60.17 kJ/mol in the absence and presence of oxygen, respectively. These results indicate that the CO_2 chemisorption in Li_5FeO_4 becomes less thermal dependent when oxygen is present in the gas mixture.

On the basis of all these results, it can be said that oxygen addition does enhance the CO_2 chemisorption on Li_5FeO_4 at $T \leq 700$ °C. At higher temperatures than 700 °C, oxygen addition seems to favor the desorption process.

CONCLUSIONS

The CO_2 capture properties of Li_5FeO_4 were theoretical and experimentally demonstrated. Results regarding ab initio thermodynamic calculations on the Li_5FeO_4–CO_2 system show the capability of the material to chemically trap CO_2 in a wide range of temperatures under different CO_2 partial pressure conditions. According to theoretical results, thermogravimetric analyses of the capture process showed the high reactivity of the material with CO_2 from 200 to 750 °C and CO_2 partial pressure values from 0.2 to 1. Besides, TGA suggests that this material is able to capture CO_2 through the same mechanism of chemisorption–desorption reported previously for other lithium-containing ceramics captors, wherein diffusion is identified as the limiting step in the whole chemisorption process. Moreover, pentalithium ferrite would be considered as an interesting alternative for CO_2 capture due to its high capture kinetics as well as high capture capacity of about 12.9 mmol/g. Additionally, the chemisorption performance observed at low CO_2 partial pressure values (P_{CO2} around 0.2) suggest the capability of the sorbent to be used under postcombustion conditions. Finally, results showed that the presence of small quantities of oxygen may enhance the CO_2 chemisorption on Li_5FeO_4 at temperatures below 700 °C, whereas at higher temperatures oxygen addition seems to promote the desorption process.

AUTHOR INFORMATION

Corresponding Author

*E-mail: pfeiffer@iim.unam.mx. Phone: +52 (55) 5622 4627. Fax: +52 (55) 5616 1371.

ORCID

Heriberto Pfeiffer: 0000-0002-6217-3420

Notes

The authors declare no competing financial interest.

ACKNOWLEDGMENTS

H.A.L.-G. and P.S.-C. thank to CONACYT for personal financial support. Authors thank to the projects SENER-CONACYT (251801) and PAPIIT-UNAM (IN-101916) for financial support and A. Tejeda for technical assistance.

REFERENCES

(1) Samanta, A.; Zhao, A.; Shimizu, G. K. H.; Sarkar, P.; Gupta, R. Post-combustion CO_2 capture using solid sorbents: A review. *Ind. Eng. Chem. Res.* **2012**, *51*, 1438–1463.

(2) Jo, H. G.; Yoon, H. J.; Lee, C. H.; Lee, K. B. Citrate sol–gel method for the preparation of sodium zirconate for high-temperature CO_2 Sorption. *Ind. Eng. Chem. Res.* **2016**, *55*, 3833–3839.

(3) Wang, J.; Huang, L.; Yang, R.; Zhang, Z.; Wu, J.; Gao, Y.; Wang, Q.; O'Hare, D.; Zhong, Z. Recent advances in solid sorbents for CO_2 capture and new development trends. *Energy Environ. Sci.* **2014**, *7*, 3478–3518.

(4) Boot-Handford, M. E.; Abanades, J. C.; Anthony, E. J.; Blunt, M. J.; Brandani, S.; Mac Dowell, N.; Fernández, J. R.; Ferrari, M.-C.; Gross, R.; Hallett, J. P. Carbon capture and storage update. *Energy Environ. Sci.* **2014**, *7*, 130–189.

(5) Kenarsari, S. D.; Yang, D.; Jiang, G.; Zhang, S.; Wang, J.; Russell, A. G.; Wei, Q.; Fan, M. Review of recent advances in carbon dioxide separation and capture. *RSC Adv.* **2013**, *3*, 22739–22773.

(6) Choi, S.; Drese, J. H.; Jones, C. W. Adsorbent materials for carbon dioxide capture from large anthropogenic point sources. *ChemSusChem* **2009**, *2*, 796–854.

(7) Valverde, J. M. Ca-based synthetic materials with enhanced CO_2 capture efficiency. *J. Mater. Chem. A* **2013**, *1*, 447–468.

(8) Lu, X.; Jin, D.; Wei, S.; Wang, Z.; An, C.; Guo, W. Strategies to enhance CO_2 capture and separation based on engineering absorbent materials. *J. Mater. Chem. A* **2015**, *3*, 12118–12132.

(9) Ochoa-Fernández, E.; Rønning, M.; Grande, T.; Chen, D. Synthesis and CO_2 capture properties of nanocrystalline lithium zirconate. *Chem. Mater.* **2006**, *18*, 6037–6046.

(10) Nakagawa, K.; Ohasi, T. A novel method of CO_2 capture from high temperature gases. *J. Electrochem. Soc.* **1998**, *145*, 1344–1346.

(11) Radfarnia, H. R.; Iliuta, M. C. Surfactant template/ultrasound assisted method for preparation of porous nanoparticle lithium zirconate. *Ind. Eng. Chem. Res.* **2011**, *50*, 9295–9305.

(12) Ochoa-Fernandez, E.; Rønning, M.; Yu, X.; Grande, T.; Chen, D. Compositional effects of nanocrystalline lithium zirconate on its CO_2 capture properties. *Ind. Eng. Chem. Res.* **2008**, *47*, 434–442.

(13) Durán-Muñoz, F.; Romero-Ibarra, I. C.; Pfeiffer, H. Analysis of the CO_2 chemisorption reaction mechanism in lithium oxosilicate (Li_8SiO_6): A new option for high-temperature CO_2 capture. *J. Mater. Chem. A* **2013**, *1*, 3919–3925.

(14) Quinn, R.; Kitzhoffer, R. J.; Hufton, J. R.; Golden, T. C. A high temperature lithium orthosilicate-based solid absorbent for post combustion CO_2 capture. *Ind. Eng. Chem. Res.* **2012**, *51*, 9320–9327.

(15) Xu, H.; Cheng, W.; Jin, X.; Wang, G.; Lu, H.; Wang, H.; Chen, D.; Fan, B.; Hou, T.; Zhang, R. Effect of the particle size of quartz powder on the synthesis and CO_2 absorption properties of Li_4SiO_4 at high temperature. *Ind. Eng. Chem. Res.* **2013**, *52*, 1886–1891.

(16) Amorim, S. M.; Domenico, M. D.; Dantas, T. L. P.; José, H. J.; Moreira, R. F. P. M. Lithium orthosilicate for CO_2 capture with high regeneration capacity: kinetic study and modeling of carbonation and decarbonation reactions. *Chem. Eng. J.* **2016**, *283*, 388–396.

(17) Avalos-Rendón, T.; Casa-Madrid, J.; Pfeiffer, H. Thermochemical capture of carbon dioxide on lithium aluminates ($LiAlO_2$ and Li_5AlO_4): A new option for the CO_2 absorption. *J. Phys. Chem. A* **2009**, *113*, 6919–6923.

(18) Matsukura, Y.; Okumura, T.; Kobayashi, R.; Oh-ishi, K. Synthesis and CO_2 absorption properties of single-phase Li_2CuO_2 as a CO_2 absorbent. *Chem. Lett.* **2010**, *39*, 966–967.

DOI: 10.1021/acs.jpcc.6b12431
J. Phys. Chem. C 2017, 121, 3455–3462

(19) Oh-Ishi, K.; Matsukura, Y.; Okumura, T.; Matsunaga, Y.; Kobayashi, R. Fundamental research on gas-solid reaction between CO_2 and Li_2CuO_2 linking application for solid CO_2 absorbent. *J. Solid State Chem.* **2014**, *211*, 162−169.
(20) Lara-García, H. A.; Alcantar-Vazquez, B.; Duan, Y.; Pfeiffer, H. CO chemical capture on L_2CuO_2, through a consequtive CO oxidation and chemisorption bifunctional process. *J. Phys. Chem. C* **2016**, *120*, 3798−3806.
(21) Ueda, S.; Inoue, R.; Sasaki, K.; Wakuta, K.; Ariyama, T. CO_2 absorption and desorption abilities of Li_2O-TiO_2 compounds. *ISIJ Int.* **2011**, *51*, 530−537.
(22) Ortiz-Landeros, J.; Ávalos-Rendón, T. L.; Gómez-Yánez, C.; Pfeiffer, H. Analysis and perspectives concerning CO_2 chemisorption on lithium ceramics using thermal analysis. *J. Therm. Anal. Calorim.* **2012**, *108*, 647−655.
(23) López-Ortiz, A.; Escobedo-Bretado, M. A.; Guzmán-Velderrain, V.; Meléndez-Zaragoza, M.; Salinas-Gutiérrez, J.; Collins-Martínez, V. Experimental and modeling kinetic study of the CO_2 absorption by Li_4SiO_4. *Int. J. Hydrogen Energy* **2014**, *39*, 16656−16666.
(24) Takeshita, H.; Ohmichi, T.; Nasu, S.; Watanabe, H.; Sasayama, A.; Mass, A. Spectrometric study of the evaporation of Li_5FeO_4 as a corrosion product in the compatibility experiment of Li_2O pellets with Fe-Ni-Cr alloys. *J. Nucl. Mater.* **1978**, *78*, 281−288.
(25) Hirano, A.; Matsumura, T.; Ueda, M.; Imanishi, N.; Takeda, Y.; Tabuchi, M. Electrochemical properties and mössbauer effect of anti-fluorite type compound Li_5FeO_4. *Solid State Ionics* **2005**, *176*, 2777−2782.
(26) Liang, L.; Luo, J.; Chen, M.; Wang, L.; Li, J.; He, X. Synthesis and characterization of novel cathode material Li_5FeO_4 for Li-ion batteries. *Inter. J. Electrochem. Sci.* **2013**, *8*, 6393−6398.
(27) Johnson, C. S.; Kang, S. H.; Vaughey, J. T.; Pol, S. V.; Balasubramanian, M.; Thackeray, M. M. Li_2O removal from Li_5FeO_4: A cathode precursor for lithium-ion batteries. *Chem. Mater.* **2010**, *22*, 1263−1270.
(28) Martın, F.; Navarrete, E.; Morales, J.; Roldán, C.; Ramos-Barrado, J. R.; Sánchez, L. High-energy, efficient and transparent electrode for lithium batteries. *J. Mater. Chem.* **2010**, *20*, 2847−2852.
(29) Li, K.; Chen, H.; Shua, F.; Chen, K.; Xue, D. Low temperature synthesis of Fe_2O_3 and $LiFeO_2$ as cathode materials for lithium-ion batteries. *Electrochim. Acta* **2014**, *136*, 10−18.
(30) Yanase, I.; Kameyama, A.; Kobayashi, H. CO_2 absorption and structural phase transition of α-$LiFeO_2$. *J. Ceram. Soc. Jpn.* **2010**, *118*, 48−51.
(31) Kato, M.; Essaki, K.; Nakagawa, K.; Suyama, Y.; Terasaka, K. CO_2 absorption properties of lithium ferrite for application as a high-temperature CO_2 absorbent. *J. Ceram. Soc. Japan* **2005**, *113*, 684−686.
(32) Gómez-García, F.; Pfeiffer, H. Structural and CO_2 capture analyses of the $Li_{1+x}FeO_2$ ($0 \leq x \leq 0.3$) system: effect of different physicochemical conditions. *RSC Adv.* **2016**, *6*, 112040−112049.
(33) Duan, Y.; Sorescu, D. C. Density functional theory studies of the structural, electronic, and phonon properties of Li_2O and Li_2CO_3: Aplication to CO_2 capture reaction. *Phys. Rev. B: Condens. Matter Mater. Phys.* **2009**, *79*, 014301.
(34) Duan, Y. ab initio thermodynamic approach to identify mixed solid sorbents for CO_2 capture technology. *Front. Environ. Sci.* **2015**, *3*, 69−74.
(35) Duan, Y.; Lekse, J.; Wang, X.; Li, B.; Alcantar-Vazquez, B.; Pfeiffer, H.; Halley, J. W. Electronic structure, phonon dynamical properties, and capture capability of $Na_{2-x}M_xZrO_3$ (M = Li,K): Density-functional calculations and experimental validations. *Phys. Rev. Appl.* **2015**, *3*, 044013.
(36) Cox, D. E.; Takei, W. J.; Shirane, G. The magnetic structure of ordered and disordered $LiFeO_2$. *American Crystallographic Association: Program and Abstracts* **1962**, 6−6.
(37) Luge, R.; Hoppe, R. News on oxoferrates(Iii). On Li_5FeO_4 (with a remark on $Na_5Fe_{1-x}Ga_xO_4$ solid-solutions). *Z. Anorg. Allg. Chem.* **1984**, *513*, 141−150.
(38) Kresse, G.; Hafner, J. ab initio molecular-dynamics for liquid-metals. *Phys. Rev. B: Condens. Matter Mater. Phys.* **1993**, *47*, 558−561.
(39) Kresse, G.; Furthmuller, J. Efficiency of ab-initio total energy calculations for metals and semiconductors using a plane-wave basis set. *Comput. Mater. Sci.* **1996**, *6*, 15−50.
(40) Parlinski, K. *Software PHONON* 2006, http://www.computingformaterials.com (accessed September, 2016).
(41) Lowell, S.; Shields, J. E.; Thomas, M. A. *Characterization of Porous Solids and Powders: Surface Area, Pore Size and Density*; Kluwer Academic Publishers: London, 2004.
(42) Pfeiffer, H.; Bosch, P. Thermal stability and high-temperature carbon dioxide sorption on hexa-lithium zirconate ($Li_6Zr_2O_7$). *Chem. Mater.* **2005**, *17*, 1704−1710.
(43) Zhao, T.; Ronning, M.; Chen, D. Preparation of nanocrystalline Na_2ZrO_3 for high-temperature CO_2 acceptors: chemistry and mechanism. *J. Energy Chem.* **2013**, *22*, 387−393.
(44) Zheng, Q.; Huang, L.; Zhang, Y.; Wang, J.; Zhao, C. Z.; Zhang, Q.; Zheng, W.; Cao, D.; O'Hare, D.; Wang, Q. Unexpected highly reversible topotactic CO_2 sorption/desorption capacity for potassium dititanate. *J. Mater. Chem. A* **2016**, *4*, 12889−12896.
(45) Kim, H.; Jang, H. D.; Choi, M. Facile synthesis of macroporous Li_4SiO_4 with remarkably enhanced CO_2 adsorption kinetics. *Chem. Eng. J.* **2015**, *280*, 132−137.
(46) Wang, K.; Yin, Z.; Zhao, P. Synthesis of macroporous Li_4SiO_4 via a citric acid-based sol-gel route coupled with carbon coating and its CO_2 chemisorption properties. *Ceram. Int.* **2016**, *42*, 2990−2999.
(47) Lara-García, H. A.; Pfeiffer, H. High and efficient Li_2CuO_2-CO_2 chemisorption using different partial pressures and enhancement produced by the oxygen addition. *Chem. Eng. J.* **2016**, DOI: 10.1016/j.cej.2016.11.029.

DOI: 10.1021/acs.jpcc.6b12431
J. Phys. Chem. C 2017, 121, 3455−3462